

1N-27  
2698  
g24

# Crystallization and Properties of Sr-Ba Aluminosilicate Glass- Ceramic Matrices

Narottam P. Bansal and Mark J. Hyatt  
*Lewis Research Center*  
*Cleveland, Ohio*

Charles H. Drummond, III  
*Ohio State University*  
*Columbus, Ohio*

Prepared for the  
15th Annual Conference on Composites and Advanced Ceramics  
sponsored by the American Ceramic Society  
Cocoa Beach, Florida, January 13-16, 1991



(NASA-TM-103764) CRYSTALLIZATION AND  
PROPERTIES OF Sr-Ba ALUMINOSILICATE  
GLASS-CERAMIC MATRICES (NASA) 24 pCSCL 11C

N91-19308

Unclass  
G3/27 0002698



**CRYSTALLIZATION AND PROPERTIES OF  
Sr-Ba ALUMINOSILICATE GLASS-CERAMIC MATRICES**

**NAROTTAM P. BANSAL AND MARK J. HYATT  
National Aeronautics and Space Administration  
Lewis Research Center, Cleveland, Ohio 44135**

**CHARLES H. DRUMMOND, III\***  
**Department of Materials Science and Engineering  
The Ohio State University, Columbus, Ohio 43210**

**ABSTRACT**

Powders of roller quenched  $(\text{Sr}, \text{Ba})\text{O} \cdot \text{Al}_2\text{O}_3 \cdot 2\text{SiO}_2$  glasses of various compositions were uniaxially pressed into bars and hot isostatically pressed at 1350 °C for 4h or cold isostatically pressed and sintered at different temperatures between 800 °C to 1500 °C for 10 or 20h. Densities, flexural strengths, and linear thermal expansion were measured for three compositions. The glass transition and crystallization temperatures were determined by DSC. The liquidus and crystallization temperature from the melt were measured using high temperature DTA. Crystalline phases formed on heat treatment of the glasses were identified by powder X-ray diffraction. In Sr containing glasses, the monoclinic celsian phase always crystallized at temperatures above 1000 °C. At lower temperatures, the hexagonal analogue formed. The temperature for orthorhombic to hexagonal structural transformation increased monotonically with SrO content, from 327 °C for  $\text{BaO} \cdot \text{Al}_2\text{O}_3 \cdot 2\text{SiO}_2$  to 758 °C for  $\text{SrO} \cdot \text{Al}_2\text{O}_3 \cdot 2\text{SiO}_2$ . These glass powders can be sintered to almost

\*NASA/ASEE faculty fellow at Lewis Research Center.

full densities and monoclinic celsian phase at a relatively low temperature of 1100 °C.

## INTRODUCTION

As part of an ongoing research program at NASA Lewis to develop high-temperature ceramic matrix composites, glass of celsian composition,  $\text{BaO} \cdot \text{Al}_2\text{O}_3 \cdot 2\text{SiO}_2$ , is being investigated<sup>1-5</sup>. The high melting point (1760 °C), low thermal expansion ( $2.29 \times 10^{-6} / ^\circ\text{C}$ ), and good oxidation resistance of celsian offer great promise as a suitable matrix for reinforcement with high modulus ceramic fibers. Unfortunately, the high temperature phase, hexacelsian, forms metastably in this glass at all temperatures including those below 1590 °C, the temperature for celsian to hexacelsian transformation. The kinetics<sup>6</sup> of hexacelsian to monoclinic celsian phase transformation is very slow. In addition, hexacelsian undergoes a reversible transformation into an orthorhombic structure at ~300°C accompanied by a volume change which makes it unsuitable as a matrix material for high temperature structural composites. Previous investigators<sup>7</sup> have shown that the substitution of SrO for BaO in polycrystalline  $\text{BaO} \cdot \text{Al}_2\text{O}_3 \cdot 2\text{SiO}_2$  facilitates the hexacelsian to celsian transformation and, in fact, under certain conditions hexacelsian may never form.

The objectives of the present study were to investigate the effect of the presence of SrO in  $\text{BaO} \cdot \text{Al}_2\text{O}_3 \cdot 2\text{SiO}_2$  glass on the

physical properties such as density, thermal expansion, glass transition, and crystallization temperatures and hexacelsian to celsian phase transformation. In this paper, the monoclinic celsian ( $\text{BaAl}_2\text{Si}_2\text{O}_8$ ) phase will be referred to as celsian as will the same structure with Sr or solid solutions of the two. Likewise, the hexagonal  $\text{MAl}_2\text{Si}_2\text{O}_8$  ( $\text{M} = \text{Ba}, \text{Sr}$ ) phase will be designated as hexacelsian regardless of the composition.

## EXPERIMENTAL METHODS

### Glass Melting

Glasses of various compositions (Table I) in the  $(\text{Ba}, \text{Sr})\text{O} \cdot \text{Al}_2\text{O}_3 \cdot 2\text{SiO}_2$  system were melted at  $\sim 2000 - 2100^\circ\text{C}$  in a continuous electric melter with Mo electrodes using laboratory grade  $\text{BaCO}_3$ ,  $\text{SrCO}_3$ ,  $\text{Al}_2\text{O}_3$ , and  $\text{SiO}_2$ . A well blended mixture of the starting materials of the stoichiometric composition  $\text{BaO} \cdot \text{Al}_2\text{O}_3 \cdot 2\text{SiO}_2$  was continuously fed into the furnace, the molten glass was continuously withdrawn through a manually controlled needle valve, and was quickly quenched, resulting in homogeneous, clear, and colorless flakes or rods of glass. The glass composition was changed by charging powders of increasing SrO content. The flakes were wet ground in an attrition mill using zirconia or alumina media, resulting in fine glass powder having an average particle diameter of  $\sim 2.5\mu\text{m}$ .

### Chemical Analysis

The Ba, Sr, Al, and Si contents in the glasses were

determined from wet chemical analysis and Mo by spectrographic technique. The estimated uncertainties of the two methods were  $\pm 1\%$  and  $\pm 10\%$ , respectively. The analyzed glass compositions are given in Table I. The presence of  $\text{MoO}_3$  is probably due to the Mo electrodes used in electric melting of the glasses.

### **Heat Treatments**

Heat treatments of the glasses were carried out in air using a programmable Lindberg box furnace with temperature control to better than  $\pm 5^\circ\text{C}$  of the set value.

### **Cold Isostatic Pressing (CIP), Hot Isostatic Pressing (HIP), and Sintering**

Glass powders were uniaxially cold-pressed at 5,000 psi into 7.9 mm x 5.5 mm x 55 mm rectangular bars. Some of the bars were CIP'd at 60,000 psi and sintered at various temperatures between  $800^\circ\text{C}$  and  $1500^\circ\text{C}$  for 10 or 20 h in air. Other bars were HIP'd at  $1350^\circ\text{C}$  for 4 h under 45,000 psi of argon gas. Some samples were CIP'd and HIP'd.

### **Density**

Bulk densities were determined from weights and physical dimensions of the sintered specimens. Apparent densities were measured by the immersion method using water.

### **Thermal Expansion Coefficient**

The linear thermal expansion coefficient ( $\alpha$ ) and softening point of the glass were measured in static air on a glass rod about 1-in. long using an Orton automated recording dilatometer

at a heating rate of 3 °C/min. The linear thermal expansion coefficient was also determined using a Perkin-Elmer thermal mechanical analyzer TMA-7.

#### **Flexural Strength**

The flexural strength of the sintered bars was measured in 3-point bending using an Instron machine. The span length of the test bars was 1.25 in. All tests were run at a crosshead speed of 0.05 inch/min.

#### **Differential Scanning Calorimetry (DSC)**

Glass transition ( $T_g$ ) and crystallization ( $T_c$ ) temperatures of the glasses were determined from DSC performed on powder samples using a Stanton-Redcraft DSC 1500 system which was interfaced with a computer data acquisition and analysis system. About 35 - 50 mg of the glass sample contained in a platinum DSC pan was scanned from ambient temperature to 1500 °C at a heating rate of 20 °C/min. Dry argon or nitrogen flowed through the DSC cavity during the measurements.

#### **High-Temperature Differential Thermal Analysis (DTA)**

The liquidus and crystallization temperature from the melt were determined using a Netzsch Thermal Analyzer STA 429 with a Super Kanthal heating element furnace. DTA runs were made on glass powder samples at a heating rate of 10 °C/min. in an atmosphere of helium.

#### **X-ray Diffraction (XRD)**

Crystalline phases present in the heat-treated glass samples

were identified from XRD patterns recorded at room temperature using a step-scan procedure ( $0.03^\circ/2\theta$  step, count time 0.4 s) on a Philips ADP-3600 automated diffractometer equipped with a crystal monochromator employing copper  $K_\alpha$  radiation.

### Scanning Electron Microscopy

Microstructures of the fracture surfaces of the samples sintered at various temperatures were observed in a JEOL JSM-840A scanning electron microscope (SEM). A thin layer of gold was deposited onto the sample surface before viewing in the SEM.

### RESULTS AND DISCUSSION

The liquidus on heating the glasses which crystallized and the crystallization temperature on cooling the glass melt were obtained from high temperature DTA runs. The results for various glass compositions are shown in the phase diagram (Figure 1) taken from reference 7. The liquidus values are in reasonable agreement with those of Talmy and Haught<sup>7</sup>. There is little change in the liquidus value of about  $1675^\circ\text{C}$  with composition. The results of Talmy and Haught<sup>7</sup> are from starting members of the monoclinic phase, whereas the present results are from crystallization of the glasses. The temperature at which crystallization initiates from the melt at a cooling rate of  $10^\circ\text{C}/\text{min}$  is  $\sim 1450^\circ\text{C}$  for the compositions studied. This indicates that the melt had supercooled by more than  $200^\circ\text{C}$  before



crystallization. Again there was little change in the crystallization temperature with composition.

A series of DSC scans for the bulk SAS composition is shown in Figure 2. A sample of the bulk SAS glass was heated at 20 °C/min to 1300 °C in argon and fast quenched in the DSC. The  $T_g$  of the glass is 883 °C and crystallization to hexacelsian occurred at 1086 °C. When the quenched sample was reheated (second run), an endothermic peak for the orthorhombic to hexagonal phase transformation appeared with an onset temperature of 758 °C, which is significantly higher than the transformation temperature of 300 °C for the barium analogue. At some higher temperature the hexacelsian transformed to celsian, but no thermal event corresponding to this transformation appeared in the DSC scan and, in fact, none was observed in any other DSC scan in the present study. From 1300 °C, the specimen was fast quenched to room temperature again in the DSC. On reheating (third run) this quenched sample, the peak corresponding to the orthorhombic to hexagonal structural change was absent as the hexacelsian had already transformed into monoclinic phase during the second run. These results were further verified by XRD of the DSC samples.

The variation in the orthorhombic to hexagonal transformation temperature as a function of composition is shown in Figure 3. The temperature increases monotonically with composition from 327 °C for  $\text{BaO} \cdot \text{Al}_2\text{O}_3 \cdot 2\text{SiO}_2$  to 758 °C for

$\text{SrO} \cdot \text{Al}_2\text{O}_3 \cdot 2\text{SiO}_2$ . The reason for this increase is not understood, although increasing SrO content does favor formation of the monoclinic phase.

In the SAS glass, only by crystallizing at temperatures less than 1000 °C can the hexacelsian phase be formed. Heat treatment of the SAS glass at higher temperatures resulted in crystallization of the monoclinic phase. In mixed glass compositions containing both SrO and BaO, the hexagonal phase can form at higher crystallization temperatures. In BAS glass, both monoclinic and hexacelsian phases were present below 1590 °C, the equilibrium temperature for monoclinic to hexagonal phase transformation. As has been previously reported<sup>2,4</sup>, the transformation of the metastable hexacelsian into the stable monoclinic phase is very sluggish and readily occurs only in the presence of an additive. The absence of any peak in a DSC scan for the hexagonal to monoclinic transformation is very puzzling. Perhaps the enthalpy change accompanying this transformation is too small to be detected in the DSC, although this does not seem likely.

The effect of glass composition on crystallization temperature,  $T_c$ , as determined by DSC at a scan rate of 20 °C/min is presented in Figure 4. The  $T_c$  is essentially constant at ~1040 °C. In all the glass compositions shown, hexacelsian crystallized except in SAS glass, which crystallized as the monoclinic phase under these conditions. Also shown in Figure 4

is the glass transition temperature,  $T_g$ , for various compositions. The  $T_g$  value of 900 °C is almost independent of the glass composition.

The linear thermal expansion,  $\alpha$ , of various phases formed with heat treatment in the SAS and BAS glass compositions are given in Table II. The corresponding  $\alpha$  values available from literature are also listed. The higher  $\alpha$  values for the hexagonal and orthorhombic phases than for the monoclinic phase for both compositions make these phases less desirable as matrix materials for fiber-reinforced composites for high temperature structural applications. The more important consideration for structural applications, however, is the volume change accompanying the orthorhombic to hexagonal transformation.

In Table III the properties of the glass powder bars of different compositions sintered under various conditions are summarized. The bars were heat treated at temperatures between 800 °C and 1500 °C for 10 or 20 h. The bulk density ( $\rho$ ) values are shown as the percent theoretical density. Theoretical densities of the mixed compositions were calculated as a weighted average of the end members. Samples sintered at 800 °C had low densities indicating almost no viscous flow or densification. Most of the sintering had occurred at 900 °C yet a small increase in density was observed at 1100 °C. Densities of samples heat treated at 1300 and 1500 °C were lower, probably due to grain growth and grain coarsening as seen below in the

SEM microstructures of the fracture surfaces of these specimens. There was no attempt to optimize the sintered density; however, a heat treatment at 1100 °C for 20 h gave the highest densities for all compositions. The crystalline phases identified from XRD are also shown. For the SrO containing glasses, hexacelsian crystallized only at lower temperatures. At 800 °C no crystallization was detected by XRD. At 900 °C a mixture of hexacelsian and the monoclinic phases was present. At all higher temperatures only the monoclinic phase was detected by XRD. Limited flexural strength measurements on only two bars under each sintering condition were made, and moderate values of 13 - 19 ksi were obtained.

Typical powder XRD patterns of glass powders of SR1, SR3, and SAS compositions CIP'd at 60,000 psi and sintered in air for 20 h at 900 °C or 1100 °C are shown in Figures 5 and 6, respectively. In specimens sintered at 900 °C, only the hexagonal phase is formed in SR1, whereas both hexagonal and monoclinic phases are present in SR3 and SAS compositions. Also, the fraction of monoclinic phase increased with increasing SrO content in the glass, as seen from the relative peak heights in the XRD patterns. In the 1100 °C heat-treated specimens, only the monoclinic phase is formed in all three compositions. These results are consistent with the observation that celsian formation is facilitated by increasing the SrO content. For the BAS glass, similar heat treatment at 900 °C would result in the

crystallization<sup>3</sup> of hexacelsian and at 1100 °C, a mixture of celsian and hexacelsian will form.

Typical SEM micrographs of fracture surfaces of glass powder bars of SR1 and SAS compositions sintered for 20 h at various temperatures in air are shown in Figure 7. Samples heat treated at 800 °C have very small grains but large porosity, as expected. The 900 °C and 1100 °C sintered specimens are almost free of pores and the grain size is still small. Large grain growth is observed in the 1500 °C sintered samples probably due to Ostwald ripening resulting in large pores. These SEM microstructures are in accordance with the density results of Table III. The microstructures of fracture surfaces of glass powder bars of different compositions sintered at 1500 °C for 20 h are presented in Figure 8. Again the volume fraction of porosity is relatively large in all these specimens, as expected from their measured densities.

The results of a preliminary study for the HIP'd samples are presented in Table IV. As would be expected, densities close to theoretical values were obtained. Only the monoclinic phase was detected by XRD. There appears to be no difference between samples that were uniaxially cold pressed or CIP'd prior to HIP'ing. Previous work<sup>4</sup> had suggested that CIP'ing might aid in the formation of the monoclinic phase.

#### **SUMMARY OF RESULTS**

The liquidus, crystallization, and glass transition temperatures were independent of composition for the  $(\text{Sr},\text{Ba})\text{O} \cdot \text{Al}_2\text{O}_3 \cdot 2\text{SiO}_2$  glasses. Furthermore, there was little change in the thermal expansion of the monoclinic celsian phase in the presence of  $\text{SrO}$ . The orthorhombic to hexagonal transformation temperature increased monotonically with increase in  $\text{SrO}$  content, from  $327^\circ\text{C}$  for  $\text{BaAl}_2\text{Si}_2\text{O}_8$  to  $758^\circ\text{C}$  for  $\text{SrAl}_2\text{Si}_2\text{O}_8$ . The monoclinic celsian phase always crystallized in the  $\text{Sr}$ - $\text{Ba}$  aluminosilicate and SAS glass compositions at temperatures above  $1000^\circ\text{C}$ . These glass powders can be sintered to almost full densities at a relatively low temperature of  $1100^\circ\text{C}$ .

#### CONCLUSIONS

$(\text{Sr}-\text{Ba})\text{O}-\text{Al}_2\text{O}_3-2\text{SiO}_2$  glass powders can be sintered or HIP'd to the monoclinic celsian phase with moderate matrix strengths and almost to theoretical densities. Substitution of  $\text{SrO}$  for  $\text{BaO}$  in  $\text{BaO} \cdot \text{Al}_2\text{O}_3 \cdot 2\text{SiO}_2$  glass facilitates rapid formation of the monoclinic celsian phase at lower temperatures. Thus,  $(\text{Sr}-\text{Ba})\text{O}-\text{Al}_2\text{O}_3-2\text{SiO}_2$  may be a better matrix material for high-temperature fiber-reinforced glass-ceramic matrix composites.

#### ACKNOWLEDGMENTS

The technical assistance of John Setlock, Tom Sabo, and

Ralph Garlick at NASA-Lewis is gratefully acknowledged. C. H. Drummond was a NASA/ASEE summer faculty fellow at NASA-Lewis during the course of this research.

## REFERENCES

1. Bansal, N. P. and M. J. Hyatt, "Crystallization Kinetics of BaO-Al<sub>2</sub>O<sub>3</sub>-SiO<sub>2</sub> Glasses," J. Mater. Res., 4[5] 1257-1265 (1989).
2. Bansal, N. P. and J. A. Setlock, "Silicon Carbide Fiber-Reinforced Celsian Glass-Ceramic Matrix Composites," in HITEMP Review - 1990: Advanced High Temperature Engine Materials Technology Program, NASA CP 10051, pp. 59-1 to 59-15, October 1990.
3. Hyatt, M. J. and N. P. Bansal, "Crystallization of Stoichiometric Celsian Glass Compositions," Paper No. 22-G-90, Presented at 92nd Annual Meeting Of Am. Ceram. Soc., Dallas. TX, April 1990.
4. Drummond, C. H., III, and N. P. Bansal, "Crystallization Behavior and Properties of BaO.Al<sub>2</sub>O<sub>3</sub>.2SiO<sub>2</sub> Glass Matrices," Ceram. Eng. Sci. Proc., 11[7-8] 1072-1086 (1990).
5. Drummond, C. H., III, W. E. Lee, N. P. Bansal, and M. J. Hyatt, "Crystallization of a Barium-Aluminosilicate Glass," Ceram. Eng. Sci. Proc., 10[9-10] 1485-1502 (1989).
6. Bahat, D., "Kinetic Study on the Hexacelsian-Celsian Phase Transformation," J. Mater. Sc., 5[9] 805-810 (1970).
7. Talmy, I. G. and D. A. Haught, Naval Surface Warfare Center, Silver Spring, MD (private communication).
8. Moys Corral, J. S. and A. Garcia Verduch, "The Solid Solution of Silica in Celsian," Trans. J. Brit. Ceram. Soc., 77[2] 40-44 (1978).
9. Bahat, D., "Several Metastable Alkaline-Earth Feldspar Modifications," J. Mater. Sc., 7[2] 198-201 (1972).



**Table I. Analyzed Compositions (Weight %) of Glasses in the  
(Sr,Ba)O·Al<sub>2</sub>O<sub>3</sub>·2SiO<sub>2</sub> System**

Component	BAS	SR1	SR3	SAS
BaO	39.5	26.1	13.7	0.86
SrO	N.A.	9.87	18.6	33.7
Al <sub>2</sub> O <sub>3</sub>	28.7	29.6	32.2	31.5
SiO <sub>2</sub>	31.3	34.0	35.3	33.8
Na <sub>2</sub> O	0.2	0.42	0.27	0.12
MoO <sub>3</sub>	0.01	0.01	0.01	0.01
<b>Total</b>	<b>99.7</b>	<b>100.0</b>	<b>100.08</b>	<b>100.0</b>

**Table II. Linear Thermal Expansion of Various Phases  
Crystallized in Bulk BAS/SAS Glasses on  
Heat Treatment**

Phase	Crystalline form	From TMA <sup>a</sup>		From Dilatometry	
		Temperature range	$\alpha \times 10^6 / ^\circ\text{C}$	Temperature range	$\alpha \times 10^6 / ^\circ\text{C}$
BaAl <sub>2</sub> Si <sub>2</sub> O <sub>8</sub>	Monoclinic			20-1000 °C	2.29 <sup>b</sup>
	Orthorhombic	20-300 °C	4.5	20-300 °C	7.1 <sup>b</sup>
	Hexagonal	375-905 °C	6.6	300-1000 °C	8.0 <sup>b</sup>
SrAl <sub>2</sub> Si <sub>2</sub> O <sub>8</sub>	Monoclinic	20-800 °C	2.7		
	Orthorhombic	20-600 °C	5.4	30-500 °C	7.6 <sup>c</sup>
	Hexagonal	800-900 °C	11.1	700-1000 °C	7.5 <sup>c</sup>

(a) This study

(b) Reference 8

(c) Reference 9

**Table III. Properties of Cold Pressed, CIPed (60 ksi), and Sintered Glass Bars of Various Compositions in the (Sr,Ba)O·Al<sub>2</sub>O<sub>3</sub>·2SiO<sub>2</sub> System**

Heat treatment	BAS			SR1			SR3			SAS		
	$\rho$	Phase	$\sigma$	$\rho$	Phase	$\sigma$	$\rho$	Phase	$\sigma$	$\rho$	Phase	$\sigma$
800 °C, 20 hr				64	g	0.88	63	g	0.95	66	g	0.59
900 °C, 20 hr				88	H, g	15	94	H > M	14	98	H > M, g	2.5
900 °C, 10 hr 1300 °C, 10 hr				91	M	19	93	M	18	94	M	16
900 °C, 10 hr 1300 °C, 20 hr				91	M	20	94	M	17	92	M	17
1100 °C, 20 hr				98	M	13	98	M	11	97	M	15
1300 °C, 20 hr	88	M	17	94	M	17	93	M	13	93	M	19
1500 °C, 20 hr	86	M	10	89	M	19	—	M	13	88	M	15

$\rho$ : % Theoretical density, BAS = 3.390, SR1 = 3.247, SR3 = 3.185, SAS = 3.084 g/cm<sup>3</sup>

g – Glass, H – Hexacelsian, M – Monoclinic

$\sigma$  – Bend strength (ksi)

CD-90-51392

**Table IV. Density and Crystalline Phases in Glass Bars of Two Different Compositions HIP'd at 1350 °C for 4 h under 45 ksi of Argon Gas**

System	Cold Pressed	CIP'd at 60 ksi
BAS	Monoclinic Celsian 3.335 g/cm <sup>3</sup> (98.4% theor.)	Monoclinic Celsian 3.333 g/cm <sup>3</sup> (98.3% theor.)
SAS	Monoclinic 3.064 g/cm <sup>3</sup> (99.3% theor.)	Monoclinic 3.079 g/cm <sup>3</sup> (99.8% theor.)

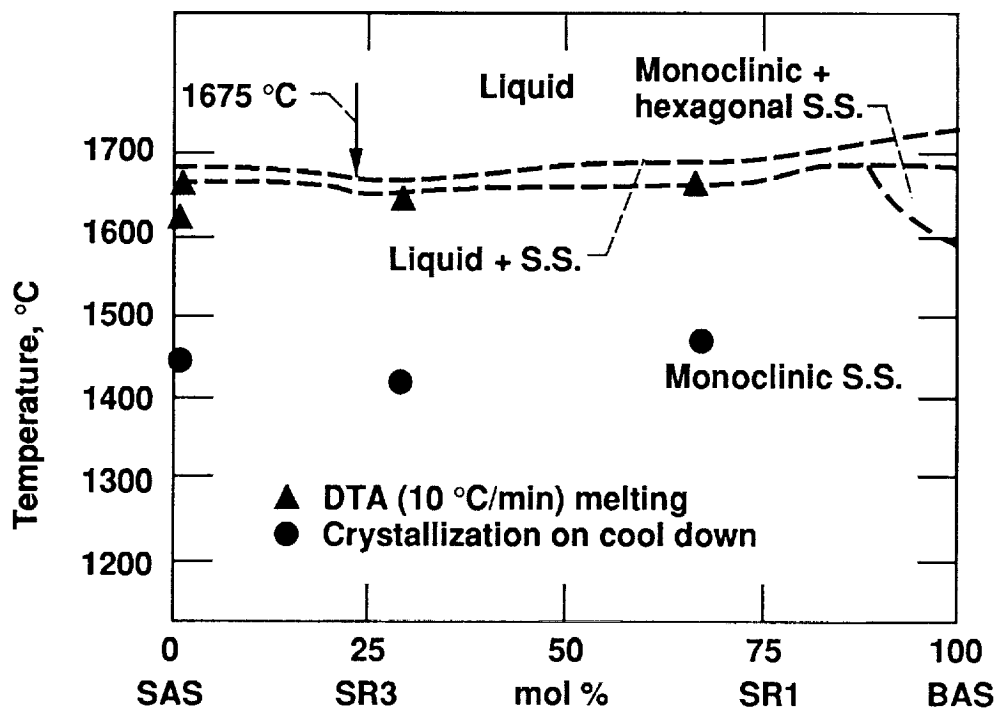


Figure 1.—Liquidus and crystallization temperatures of various compositions from high temperature DTA. (Phase diagram from Talmy and Haught<sup>7</sup>)

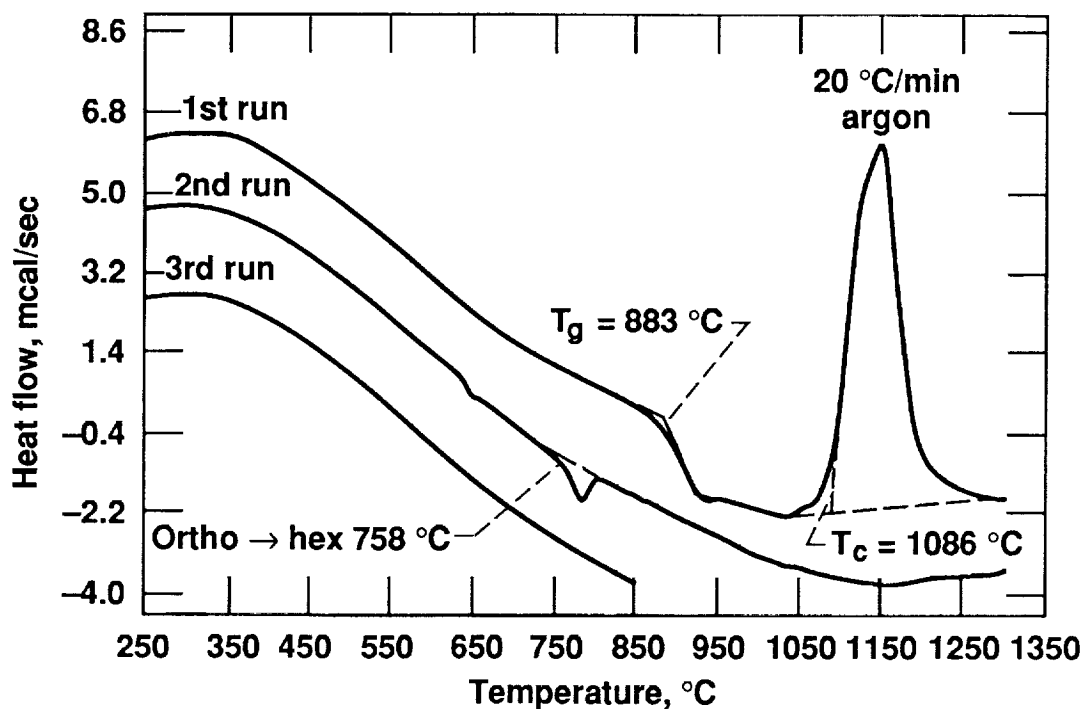


Figure 2.—Repeated DSC scans of bulk SAS glass.  $T_g$  is the glass transition temperature and  $T_c$  is the crystallization onset temperature.

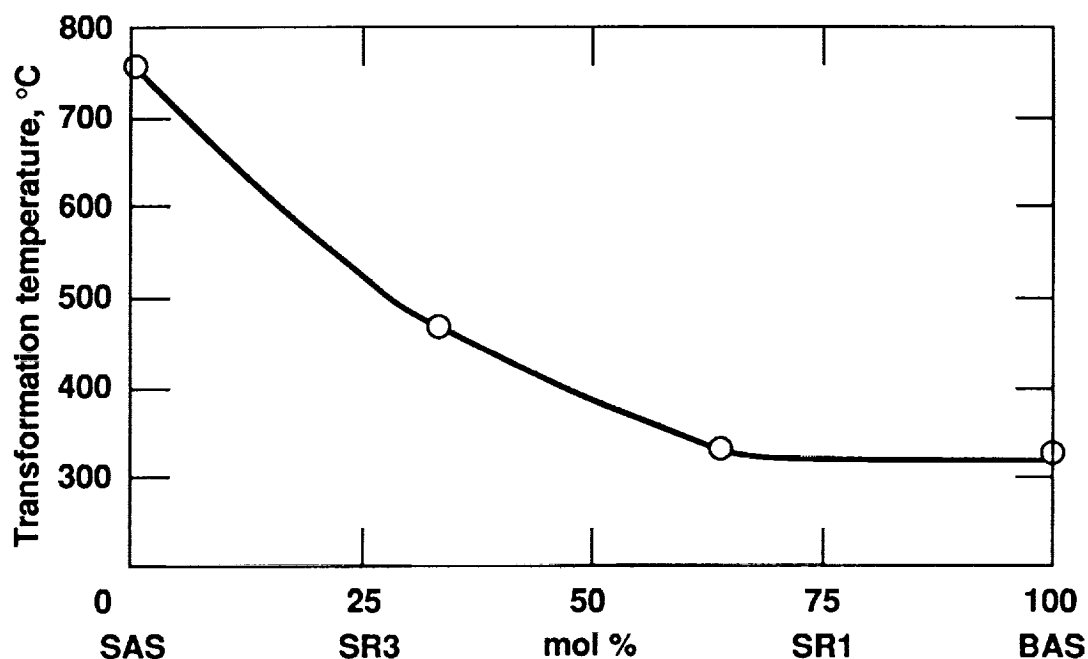


Figure 3.—Effect of composition on the orthorhombic to hexacelsian phase transformation temperature in the  $(\text{Sr}, \text{Ba}) \text{O} \cdot \text{Al}_2\text{O}_3 \cdot 2\text{SiO}_2$  system from DSC.

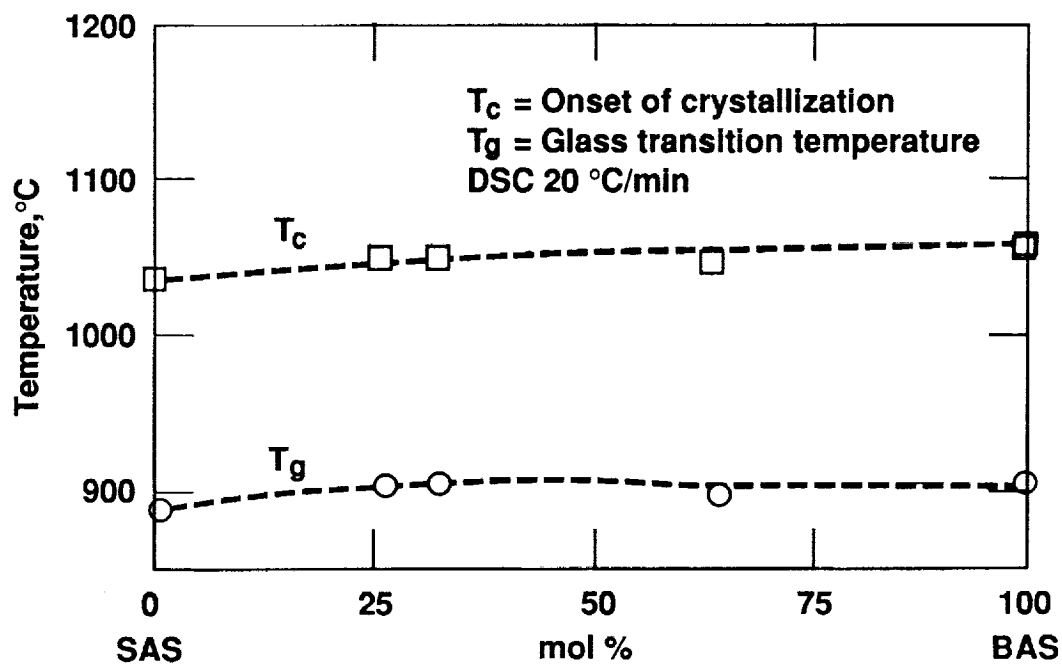


Figure 4.—Crystallization and glass transition temperatures from DSC for various glass compositions in the  $(\text{Sr}, \text{Ba}) \text{O} \cdot \text{Al}_2\text{O}_3 \cdot 2\text{SiO}_2$  system.

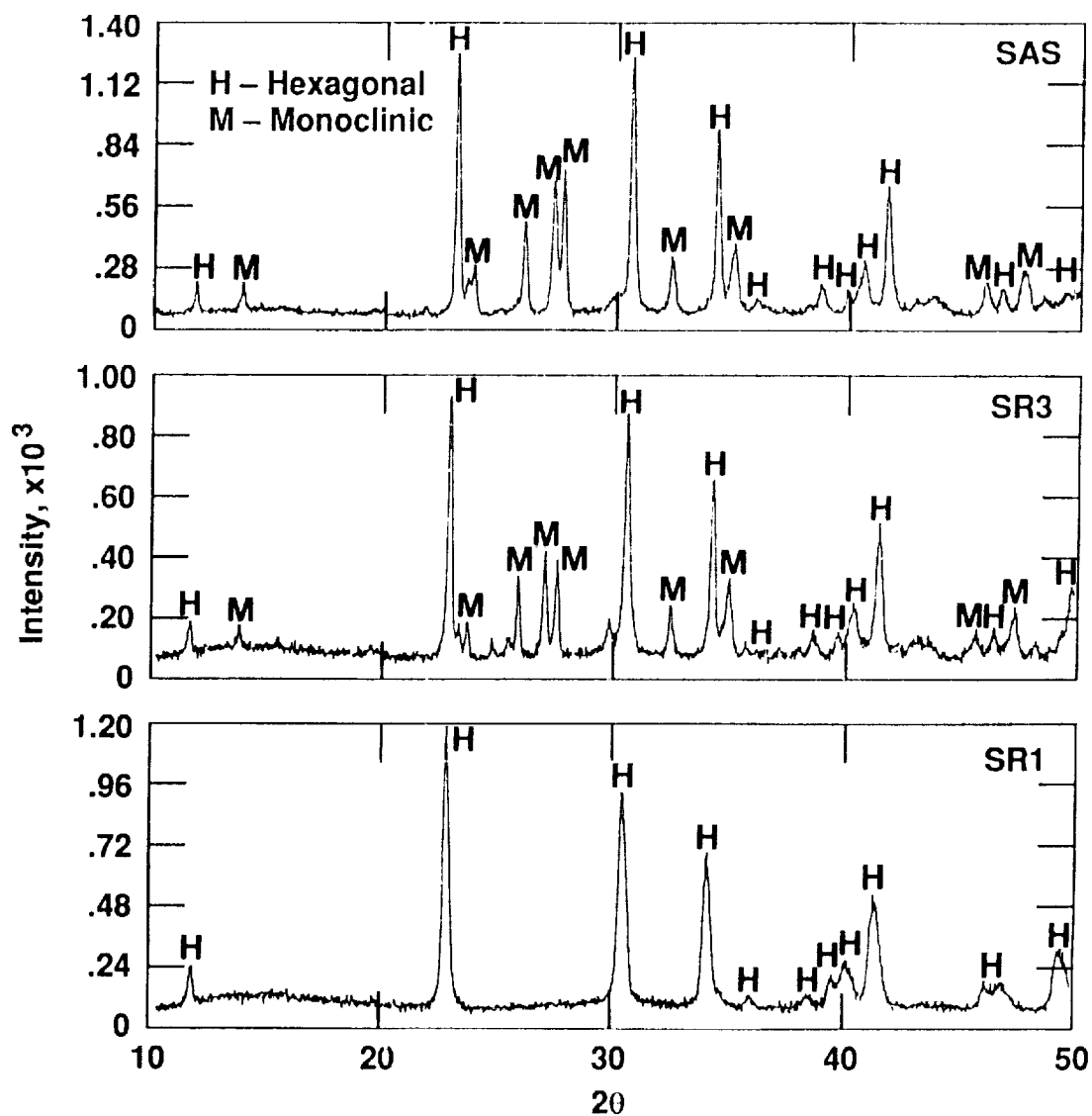


Figure 5.—Powder x-ray diffraction patterns of cold isostatically pressed and sintered (900 °C, 20 hr) glass powders of three different compositions in the  $(\text{Sr}, \text{Ba}) \text{O} \cdot \text{Al}_2\text{O}_3 \cdot 2\text{SiO}_2$  system.

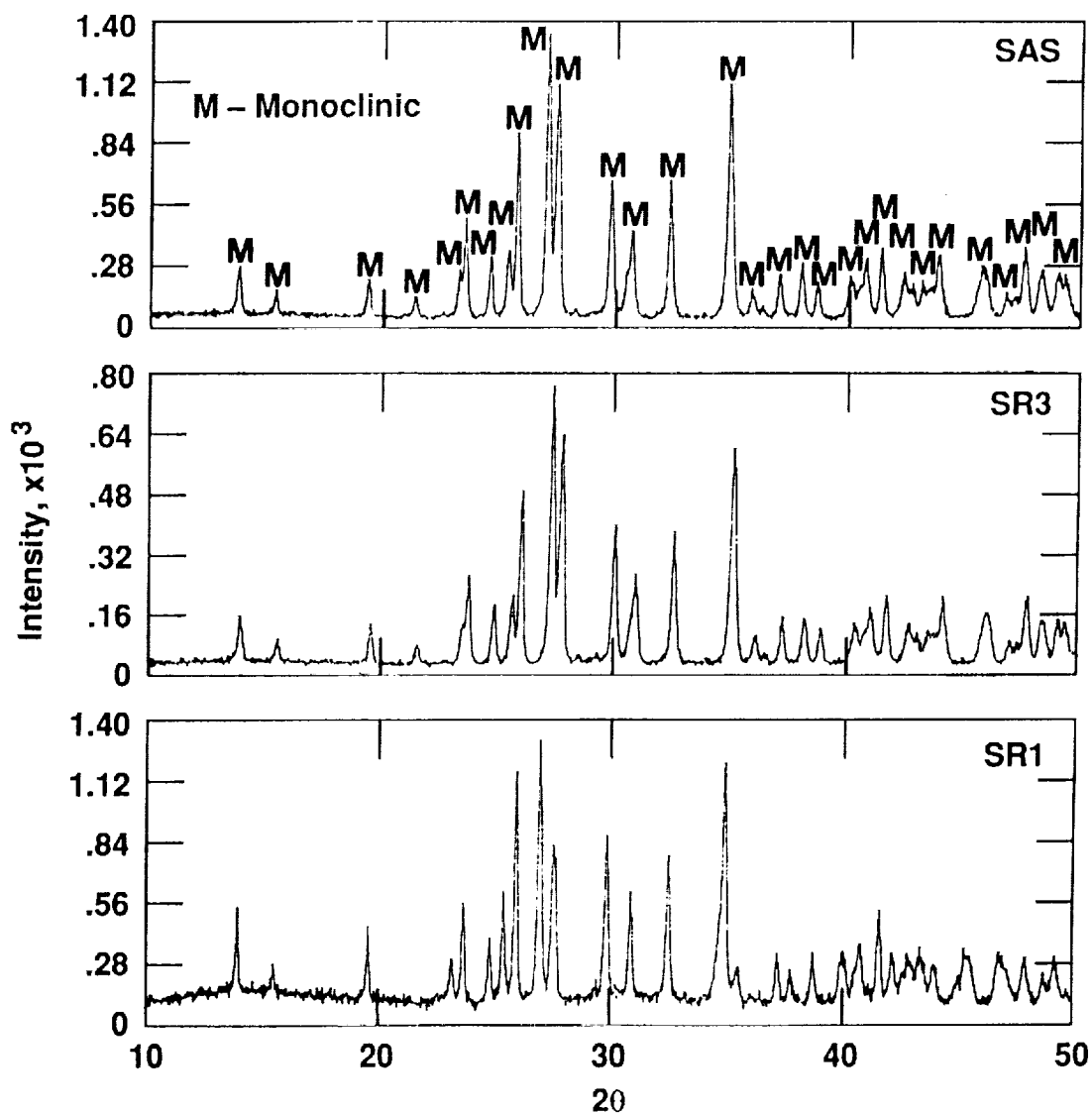


Figure 6.—Powder x-ray diffraction patterns of cold isostatically pressed and sintered (1100 °C, 20 hr) glass powders of three different compositions in the  $(\text{Sr, Ba}) \text{O} \cdot \text{Al}_2\text{O}_3 \cdot 2\text{SiO}_2$  system.

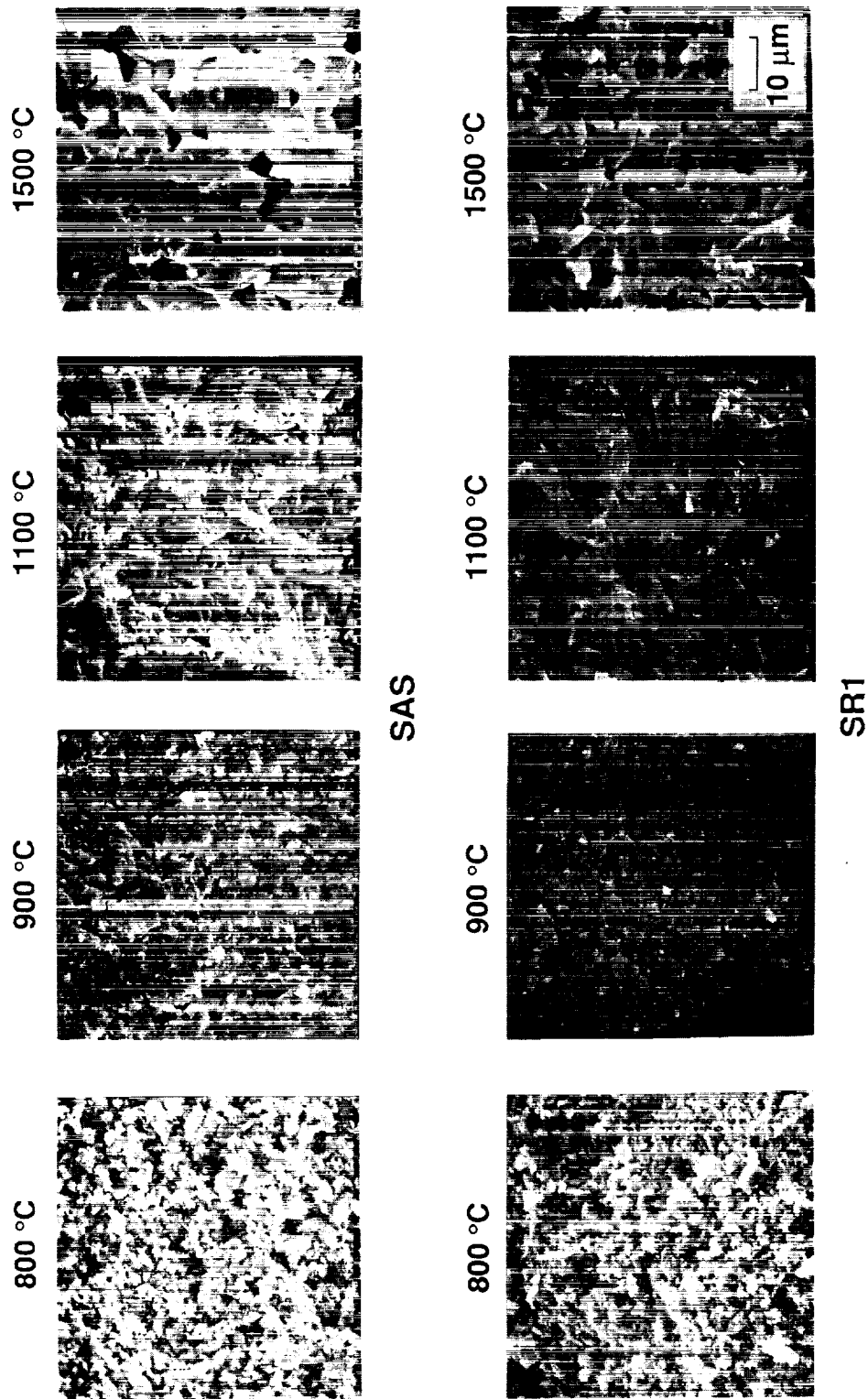
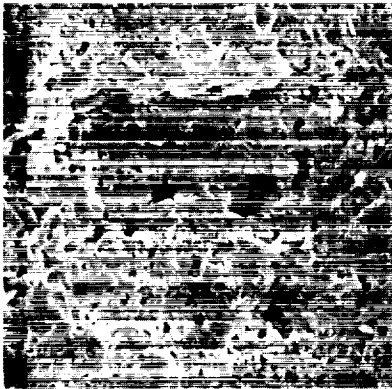
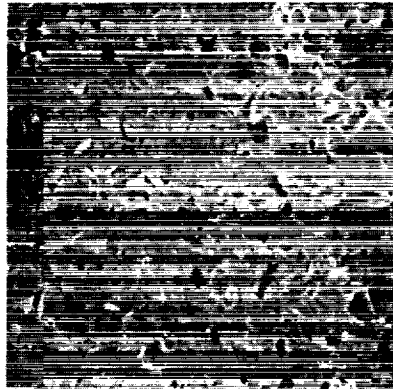


Figure 7.—SEM micrographs of fracture surfaces of SR1 and SAS glass powder bars sintered for 20 hr at various temperatures. The micron marker shown applies to all the micrographs.

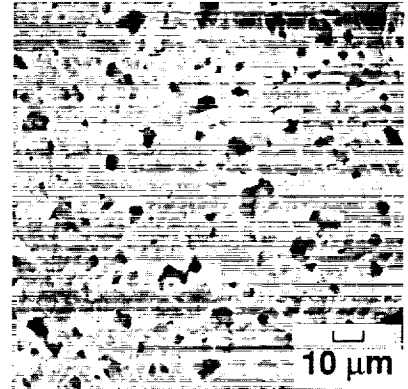
ORIGINAL PAGE IS  
OF POOR QUALITY



BAS



SR1



SAS

Figure 8.—SEM micrographs of fracture surfaces of different glass powder bars sintered at 1500 °C for 20 hr. The micron marker shown applies to all the three micrographs.



# Report Documentation Page

1. Report No. NASA TM-103764		2. Government Accession No.		3. Recipient's Catalog No.	
4. Title and Subtitle Crystallization and Properties of Sr-Ba Aluminosilicate Glass-Ceramic Matrices				5. Report Date	
				6. Performing Organization Code	
7. Author(s) Narottam P. Bansal, Mark J. Hyatt, and Charles H. Drummond, III				8. Performing Organization Report No. E-6027	
				10. Work Unit No. 510-01-01	
9. Performing Organization Name and Address National Aeronautics and Space Administration Lewis Research Center Cleveland, Ohio 44135-3191				11. Contract or Grant No.	
				13. Type of Report and Period Covered Technical Memorandum	
12. Sponsoring Agency Name and Address National Aeronautics and Space Administration Washington, D.C. 20546-0001				14. Sponsoring Agency Code	
15. Supplementary Notes Prepared for the 15th Annual Conference on Composites and Advanced Ceramics sponsored by the American Ceramic Society, Cocoa Beach, Florida, January 13-16, 1991. Narottam P. Bansal and Mark J. Hyatt, NASA Lewis Research Center; Charles H. Drummond, III, Department of Materials Science and Engineering, Ohio State University, Columbus, Ohio 43210 and NASA/ASEE faculty fellow at Lewis Research Center. Responsible person, Narottam P. Bansal, (216) 433-3855.					
16. Abstract Powders of roller quenched (Sr,Ba)O.Al <sub>2</sub> O <sub>3</sub> .2SiO <sub>2</sub> glasses of various compositions were uniaxially pressed into bars and hot isostatically pressed at 1350 °C for 4h or cold isostatically pressed and sintered at different temperatures between 800 °C to 1500 °C for 10 or 20h. Densities, flexural strengths, and linear thermal expansion were measured for three compositions. The glass transition and crystallization temperatures were determined by DSC. The liquidus and crystallization temperature from the melt were measured using high temperature DTA. Crystalline phases formed on heat treatment of the glasses were identified by powder X-ray diffraction. In Sr containing glasses, the monoclinic celsian phase always crystallized at temperatures above 1000 °C. At lower temperatures, the hexagonal analogue formed. The temperature for orthorhombic to hexagonal structural transformation increased monotonically with SrO content, from 327 °C for BaO.Al <sub>2</sub> O <sub>3</sub> .2SiO <sub>2</sub> to 758 °C for SrO.Al <sub>2</sub> O <sub>3</sub> .2SiO <sub>2</sub> . These glass powders can be sintered to almost full densities and monoclinic celsian phase at a relatively low temperature of 1100 °C.					
17. Key Words (Suggested by Author(s)) Celsian; Glass; Crystallization; Glass-ceramic; Composites; Phase transformation			18. Distribution Statement Unclassified—Unlimited Subject Category 27		
19. Security Classif. (of this report) Unclassified		20. Security Classif. (of this page) Unclassified		21. No. of pages 24	
				22. Price* A03	

